Th17 cells enhance viral persistence and inhibit T cell cytotoxicity in a model of chronic virus infection

Wanqiu Hou, Hyun Seok Kang, and Byung S. Kim

Department of Microbiology-Immunology, Feinberg School of Medicine, Northwestern University, Chicago, IL 60611

Persistent viral infection and its associated chronic diseases are a global health concern. Interleukin (IL) 17–producing Th17 cells have been implicated in the pathogenesis of various autoimmune diseases, and in protection from bacterial or fungal infection. However, the role of Th17 cells in persistent viral infection remains unknown. We report that Th17 cells preferentially develop in vitro and in vivo in an IL-6–dependent manner after Theiler's murine encephalomyelitis virus infection. Th17 cells promote persistent viral infection and induce the pathogenesis of chronic demyelinating disease. IL-17 up-regulates antiapoptotic molecules and, consequently, increases persistent infection by enhancing the survival of virus-infected cells and blocking target cell destruction by cytotoxic T cells. Neutralization of IL-17 augments virus clearance by eliminating virus-infected cells and boosting lytic function by cytotoxic T cells, leading to the prevention of disease development. Thus, these results indicate a novel pathogenic role of Th17 cells via IL-17 in persistent viral infection and its associated chronic inflammatory diseases.

CORRESPONDENCE
Byung S. Kim:
bskim@northwestern.edu

Abbreviations used: Bcl, B cell lymphoma; BMDC, BM-derived DC; CNS, central nervous system; MOI, multiplicity of infection; TMEV, Theiler's murine encephalomyelitis virus; UV-TMEV, UV light–inactivated TMEV.

When an immune response is triggered by microbial pathogens, the innate immune system directs T lymphocytes to achieve appropriate effector function from diverse pathways to protect the host against destructive invasion. However, in some cases, inappropriate T effector cells that are unable to control microbial infections are induced and expanded, thereby allowing pathogens to persist in the host. For example, the balance between Th1 and Th2 responses to an infectious agent may determine the outcome of immunoprotection versus immunopathology (1). IL-17–producing Th17 cells, which are a distinct subset of CD4$^+$ T cells, comprise another T effector cell type that is apparently involved in inflammatory tissue damage, leading to the pathogenesis of various autoimmune diseases (2–10). Furthermore, Th17 also appears to play a role in protection against extracellular bacterial or fungal diseases (11–13). The production of IL-17 has been reported during HIV infection in humans (14–17), and herpes simplex virus (18) and respiratory syncytial virus infections (19) in rodents. However, the induction of Th17 cells during persistent viral infection, and their potential roles in the establishment of viral persistence and the pathogenesis of chronic viral infection–associated diseases remain undefined.

During viral infection, most CD4$^+$ T cells isolated from the virus target organ belong to the Th1 type (1, 20). Th1 cytokines, such as IFN-γ, display strong antiviral function and antagonize the development of Th17 cells (2, 4). For example, in simian immunodeficiency virus–infected rhesus macaques, Th17 cells are markedly depleted (21). The induction of type I IFNs and their downstream signaling pathways in response to viral infection may constrain Th17 development (22, 23). In opposition to this protective strategy, a virus may be able to evade antiviral types I and II IFN responses (24), facilitating its persistence in the host by inducing elevated levels of IL-17–producing CD4$^+$ and/or CD8$^+$ T cells (25). However, the potential role of Th17 cells in the pathogenesis of virus-induced chronic inflammatory diseases is virtually unknown. Th17 cells, via their cytokine IL-17, play a pivotal role in mediating different types of tissue inflammation and destruction in chronic toxoplasmic encephalitis (26) and psoriasis (27). Therefore, it is conceivable that persistent chronic viral infection

The Journal of Experimental Medicine

might be associated with a polarized Th17 response that may further exert a positive or negative feedback loop on viral persistence and the pathogenesis of virus-induced chronic diseases.

In this study, we used the Theiler's murine encephalomyelitis virus (TMEV)–induced demyelinating disease model system, which displays immune parameters and histopathology similar to those of chronic progressive multiple sclerosis (28–30). TMEV is a natural mouse pathogen belonging to the piconavirus family, which includes many important pathogens of humans and animals; e.g., poliovirus causes paralytic disease in humans, and coxsackievirus results in mild to severe myocarditis, encephalitis, and diabetes (31). We investigated the effects of viral infection on Th17 development in vitro and in vivo, the effects of IL-17 neutralization on viral persistence in the virus target, the central nervous system (CNS), and the subsequent development of chronic demyelinating disease. In addition, we assessed the role of IL-17 in viral infection/replication and antiviral T cell cytotoxic function. Our results show that viral infection preferentially induces the development of Th17 cells, and in turn, these cells uniquely promote viral persistence via IL-17 by inhibiting apoptosis of infected cells as well as by desensitizing target cell killing by T effector cells, leading to the pathogenesis of associated chronic demyelinating disease.

RESULTS
Preferential induction of Th17 development by virus–infected DCs in vitro
To examine whether virus-infected antigen-presenting cells preferentially drive a Th17 response, purified CD4$^+$ T cells from OT-II TCR transgenic mice specific for OVA peptide 323–339 (OVA$_{323-339}$) were stimulated for 4 d with TMEV-infected BM-derived DCs (BMDCs) in the presence of the cognate peptide. Th1/Th17 cell differentiations evoked by mock- and virus-infected DCs were compared using intracellular staining of IFN-γ and IL-17, respectively (Fig. 1, A and B). The results indicate that Th17 cell development is preferentially increased after stimulation with virus-infected DCs in an infection-dose–dependent manner (Fig. 1 A). Interestingly, paraformaldehyde-fixed virus-infected DCs failed to induce polarized Th17 development (Fig. 1 B), suggesting that the skewed Th17 development is dependent on soluble factors from virus-infected DCs. To identify cytokines involved in enhanced Th17 development, key Th1/Th17 cell differentiation–associated cytokines (IL-6, IL-12, and IL-23) produced in the supernatants of virus-infected DCs were assessed (Fig. 1 C). Notably, virus-infected DCs produced higher levels of IL-6 and IL-12p40 compared with mock-infected DCs, suggesting their possible role in elevated Th17 cell differentiation. Addition of IL-6 to the co-cultures of uninfected DCs and OT-II T cells in the presence of cognate peptide promoted Th17 development (Fig. 1 D), confirming the potential role of IL-6 in Th17 elevation. In addition, treatment of the co-cultures consisting of OT-II T cells and virus-infected DCs with neutralizing antibodies to IL-6 com-

pletely abrogated Th17 development (Fig. 1 D). These results collectively indicate that IL-6 produced by virus-infected DCs likely drives Th17 cell differentiation. To directly address the effect of viral infection on virus-specific Th17 development, we used TCR transgenic SJL/J (SJL) mice (backcross generation N14) that recognize TMEV capsid protein 2 epitope (VP2$_{74-86}$) (unpublished data). Naive VP2-TCR transgenic T cells (CD4$^+$CD25$^-$CD44^{low}) sorted on a MoFlo cytometer (see Materials and methods) were used to assess the development of Th17 cells. Again, virus-infected SJL BMDCs preferentially supported the differentiation of Th17 cells, producing signature cytokines (IL-17 and IL-22) and an inflammatory cytokine (TNF-α), whereas those stimulated by BMDCs loaded with VP2$_{74-86}$– or UV light–inactivated TMEV (UV-TMEV) failed to generate Th17 cells despite the vigorous development of Th1 cells producing IFN-γ (Fig. 1 E). Thus, our data clearly demonstrate that viral infection drives antigen-presenting cells to preferentially induce Th17 development in vitro.

Elevated levels of Th17 cells in TMEV–infected susceptible mice compared with resistant mice
To determine whether persistent viral infection fosters virus-specific Th17 responses in vivo, we analyzed levels of IL-17–producing cells in the CNS of susceptible SJL and resistant C57BL/6 (B6) mice at 8 d after TMEV infection. IL-17 production by CNS-resident microglia and infiltrated macrophages, DCs, granulocytes, B cells, and cytotoxic CD8$^+$ T cells from both mouse strains was either undetectable or negligible (Fig. 2 A). However, low but detectable levels of IL-17–producing CD4$^+$ T cells were found in virus-infected SJL but not B6 mice (Fig. 2, A and C). To confirm these flow cytometry results, we assessed mRNA levels of IL-17 and the Th17 lineage–specific transcription factor RORγt in sorted CD4$^+$CD8$^-$, CD4$^-$CD8$^+$, and CD4$^-$CD8$^-$ CNS-infiltrating mononuclear cells from TMEV-infected SJL and B6 mice (Fig. 2 B). Both IL-17 and RORγt mRNAs were primarily expressed by the CD4$^+$ T cell fraction of SJL mice compared with other SJL cellular fractions (P < 0.001) or CNS-infiltrating cells from B6 mice (P < 0.001). These results clearly indicate that CD4$^+$ T cells are the predominant source of IL-17 in the CNS of virus-infected susceptible SJL mice. Th17 cell numbers in the CNS of SJL mice were as much as 100-fold greater than those of B6 mice (Fig. 2 C, bottom). In contrast, no difference in the overall number of IFN-γ–producing CD4$^+$ T cells between these strains was found as a result of elevated CD4$^+$ T cell infiltration to the CNS in SJL mice (Fig. 2 C, bottom), although the proportion of IFN-γ–producing CD4$^+$ T cells was lower in TMEV-infected SJL mice in comparison to B6 mice (Fig. 2 C, top). Th17 cells in infected SJL mice appear to be viral antigen specific, because similar levels of IL-17–producing CD4$^+$ T cells were found after in vitro stimulation with anti-CD3/CD28 versus UV-TMEV (Fig. S1, available at http://www.jem.org/cgi/content/full/jem.20082030/DC1). Upon restimulation of CNS-infiltrating cells with UV-TMEV ex vivo, significantly higher levels of

IL–17 and lower levels of IFN-γ were detected from SJL versus B6 mice (Fig. 2 D). This discrepancy between IFN-γ levels (Fig. 2 D) and IFN-γ–producing cell numbers (Fig. 2 C) may reflect differences in cytokine levels produced per cell by SJL and B6 mice. It is interesting to note that IL-6 is detectable only in the CNS (both brains and spinal cords) of SJL mice during viral infection, but not in B6 mice (Fig. 2 E), strongly suggesting that this cytokine plays a key role in Th17 development and expansion. Collectively, these observations indicate that viral infection in susceptible SJL mice results in the preferential development of Th17 responses, along with low levels of Th1 responses as compared with resistant B6 mice.
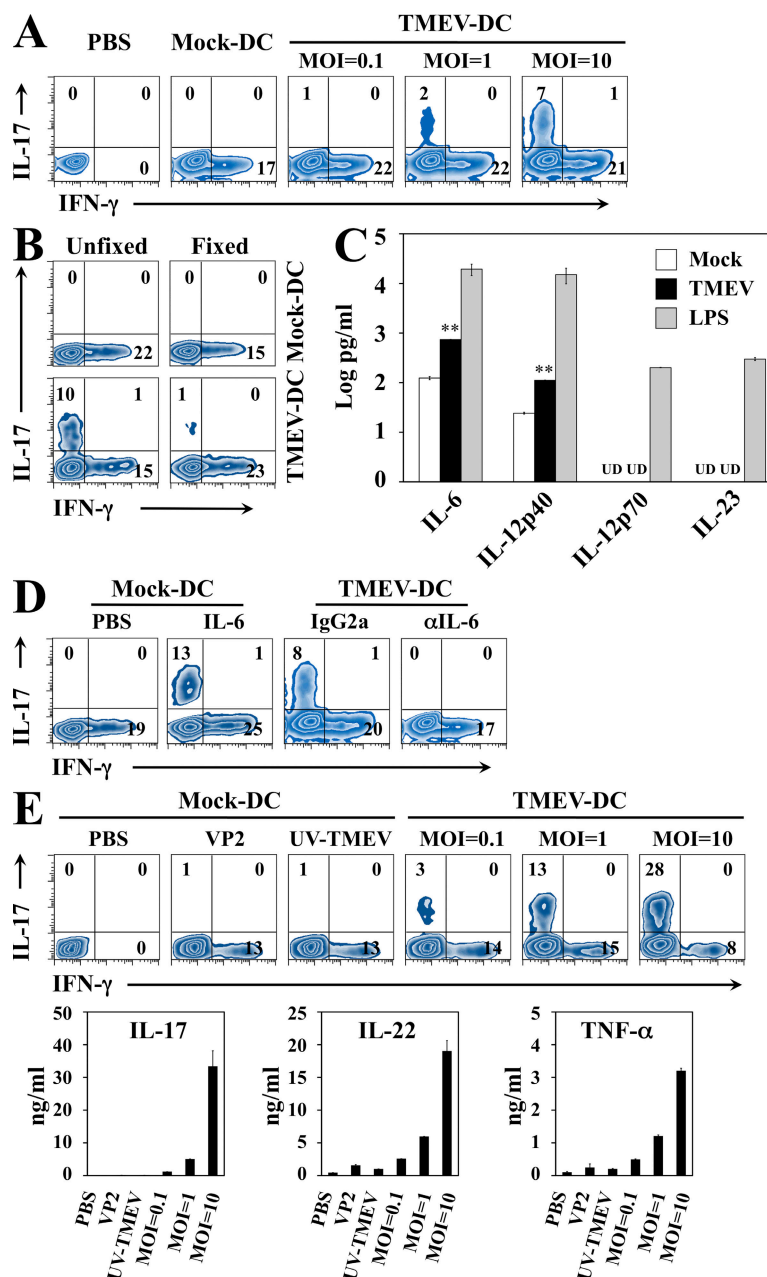

Figure 1. Virus–infected DCs promote Th17 development in vitro. (A) Flow cytometry of OT–II T cells cultured for 4 d with B6 BMDCs infected with varying MOIs in the presence of OVA$_{323-339}$. Intracellular cytokine production was determined after restimulation with PMA plus ionomycin for 6 h. (B) Flow cytometry of OT–II T cells cultured for 4 d with TMEV-infected B6 BMDCs (MOI of 10), which were treated with PBS (unfixed) or fixed with 0.1% paraformaldehyde. Plots represent gated CD4+ T cells. (C) Cytokines produced by B6 BMDCs infected with TMEV (MOI of 10) or stimulated with LPS. **, P < 0.01 versus mock. (D) Flow cytometry of OT–II T cells stimulated with OVA$_{323-339}$ in the presence of B6 BMDCs with or without IL-6, or in the presence of TMEV-infected B6 BM-DCs (MOI of 10) with either isotype or anti–IL-6 antibodies. Plots represent gated CD4+ T cells. (E) Intracellular and extracellular cytokine production by isolated naive (CD4+CD25−CD44^{low}) VP2 transgenic CD4+ T cells after stimulation with VP2$_{74-86}$– and UV-TMEV–pulsed or TMEV-infected SJL BMDCs. The data are a representative of three independent experiments (means ± SD are shown in C and E). The numbers in each quadrant represent percentages. UD, undetectable.

IL–6–dependent elevation of Th17 cell numbers in B6 mice after TMEV infection in conjunction with LPS treatment

To further correlate the observed increase in Th17 development with susceptibility to TMEV-induced demyelinating disease, we rendered resistant B6 mice susceptible by administration of the Gram–negative endotoxin LPS, as demonstrated in our earlier work (32). Intraperitoneal injection of LPS, concomitant with intracerebral TMEV infection in resistant B6

mice, resulted in persistent infection as well as clinical symptoms, whereas no detectable disease development and low viral persistence were observed in control PBS-treated mice (Fig. 3, A and B). The number of IL–17–producing CD4+ T cells in the CNS of LPS-treated mice was increased >300-fold compared with that of control PBS-treated mice (Fig. 3 C). In contrast, similar proportions and numbers of IFN-γ–producing CD4+ T cells were observed between LPS– and
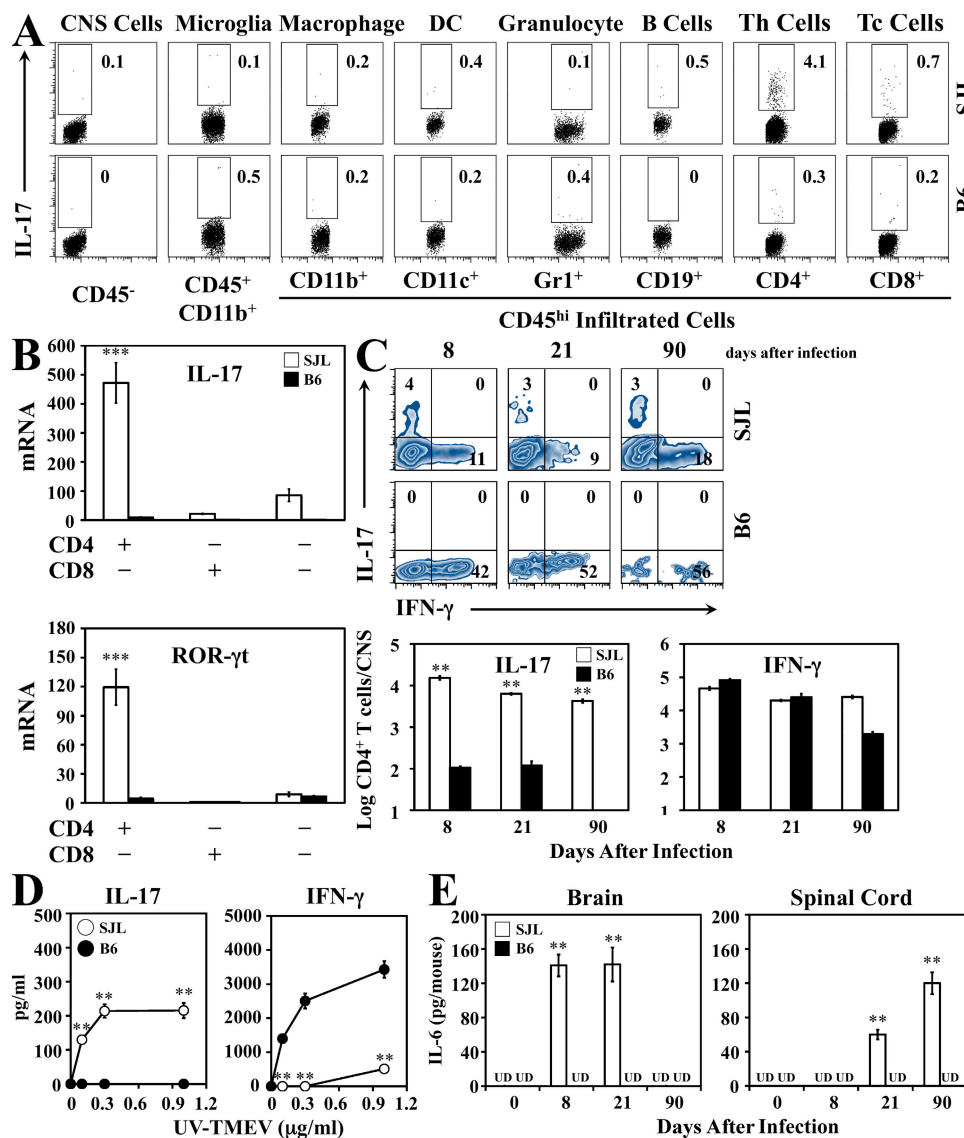
Figure 2. Th17 development is elevated in virus–infected susceptible SJL mice. (A) Intracellular IL-17 analysis of CNS mononuclear cells from virus-infected SJL and B6 mice ($n = 3$) after stimulation with PMA plus ionomycin. The number in each plot shows the proportion of IL–17–producing cells. (B) Induction of IL-17 and ROR-γt mRNAs in isolated CD4+CD8−, CD4−CD8+, and CD4−CD8− CNS mononuclear cells relative to GAPDH mRNA. Isolation of cell populations from SJL and B6 mice ($n = 6$) at 8 d after TMEV infection was achieved using a MoFlo cytometer. ***, $P < 0.001$ for SJL versus B6 mice. (C) Flow cytometry of SJL and B6 CNS-infiltrating cells from infected mice ($n = 3$), followed by stimulation with PMA plus ionomycin. Each plot is gated on CD4+ T cells (percentages are shown). The bar graphs depict cell numbers of cytokine-secreting CNS-infiltrated CD4+ T cells. **, $P < 0.01$ for SJL versus B6 mice. (D) ELISA of IL-17 and IFN-γ produced by CNS-infiltrated cells isolated from mice ($n = 3$) at 8 d after TMEV infection after stimulation with different doses of UV-TMEV. **, $P < 0.01$ for SJL versus B6 mice. (E) IL-6 levels in the CNS of SJL and B6 mice ($n = 3$) were measured by ELISA. **, $P < 0.01$ for SJL versus B6 mice. Data presented in A and C–E are representative of three independent experiments, and the results in B represent one out of two independent experiments (means ± SD are shown in B–E). UD, undetectable.

PBS-treated mice. LPS-treated mice exhibited significantly higher levels of IL-6 in particular, as well as CXCL1/KC and CCL2/MCP-1 in the brain (Fig. 3 D). These cytokines and chemokines are known to be associated with IL-17 signaling pathways (10). These results are consistent with in vitro observations that the treatment of BMDCs with LPS significantly
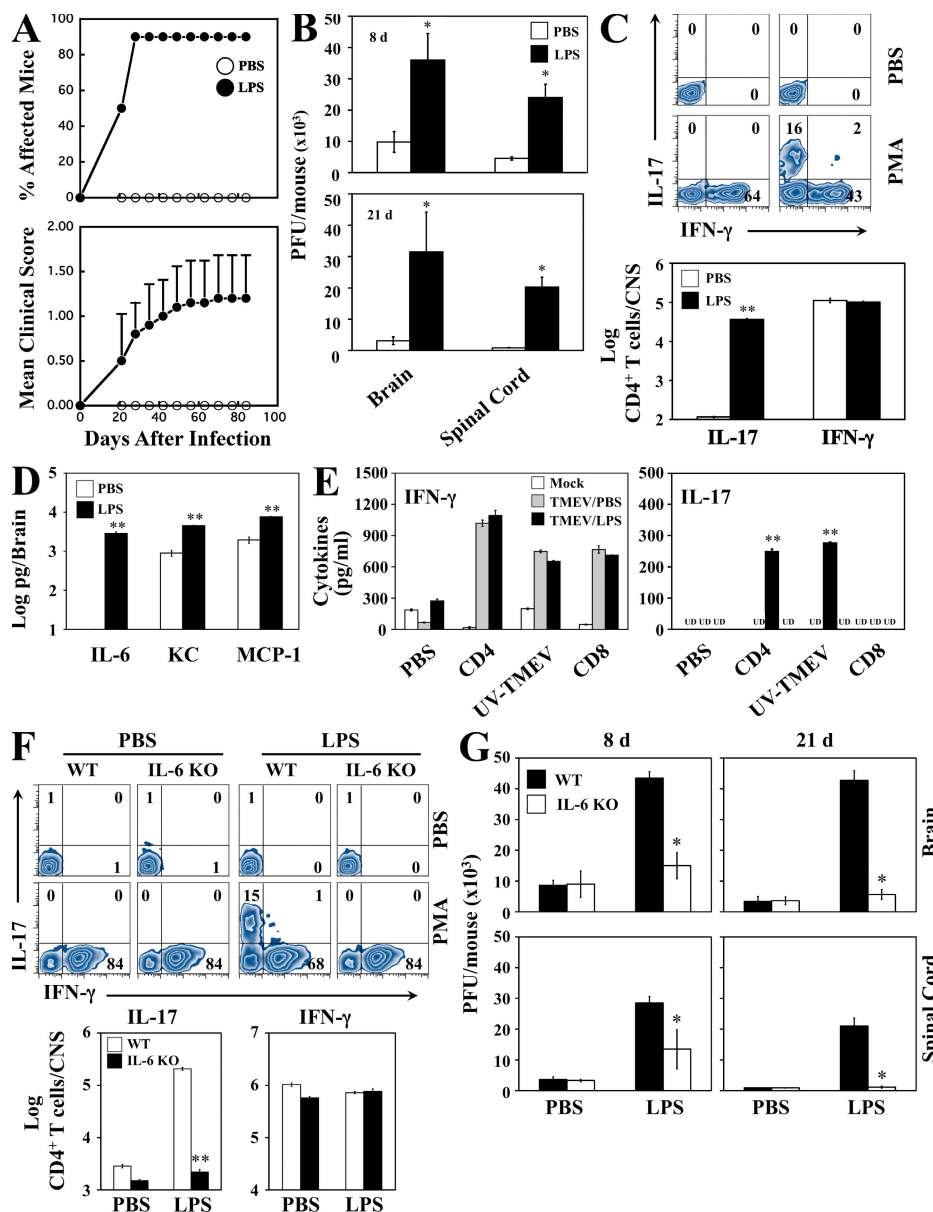
Figure 3. **Virus infection in conjunction with bacterial endotoxin administration promotes Th17 development in resistant B6 mice via elevated IL-6.** (A) B6 mice were infected with TMEV in conjunction with intraperitoneal injection of PBS ($n = 10$) or LPS ($n = 10$), and the development of demyelinating disease was monitored. One representative out of three independent experiments is shown. (B) Levels of infectious virus in the CNS were quantified 8 and 21 d after TMEV infection in PBS- or LPS-treated B6 mice. *, $P < 0.05$ between LPS- and PBS-treated groups. (C) CNS-infiltrating cells obtained at 8 d after TMEV infection from PBS- or LPS-treated mice were restimulated with PMA plus ionomycin. Plots represent gated CD4+ T cells (percentages are shown), and the graph shows numbers of cytokine-secreting CD4+ T cells. **, $P < 0.01$ between LPS- and PBS-treated groups. (D) Levels of IL-6, KC, and MCP-1 in brains were measured using ELISA 8 d after TMEV infection in PBS- or LPS-treated mice. **, $P < 0.01$ between LPS- and PBS-treated groups. (E) IFN-γ and IL-17 levels produced by splenocytes isolated from PBS- (TMEV/PBS) or LPS-treated (TMEV/LPS) B6 mice 8 d after mock or TMEV infection were assessed using ELISA after restimulation with mixed CD4 epitopes, UV-TMEV, or mixed CD8 epitopes. **, $P < 0.01$ between LPS- and PBS-treated groups. (F) CNS mononuclear cells isolated from LPS-treated WT or IL-6 KO mice at 8 d after TMEV infection were restimulated with PMA plus ionomycin. All plots show gated CD4+ T cells (percentages are shown), and the bar graphs represent numbers of cytokine-producing CD4+ T cells. **, $P < 0.01$ between WT and IL-6 KO groups. (G) Viral titers in the CNS of WT and IL-6 KO mice 8 and 21 d after infection are shown. *, $P < 0.05$ between WT and IL-6 KO groups. Results in B–G represent values from pooled CNS or spleens of two mice per group and are representative examples of three separate experiments (means ± SD are shown). UD, undetectable.

enhances the induction of Th17 cells as compared with treatment with PBS (Fig. S2, available at http://www.jem.org/cgi/content/full/jem.20082030/DC1). Thus, LPS treatment appears to be a prerequisite for Th17 elevation to the pathogenic threshold in TMEV-infected resistant B6 mice, in contrast to TMEV-infected susceptible SJL mice that generate a high level of Th17 cells. Th17 cells found in LPS-treated mice appear to represent virus-specific CD4$^+$ T cells, because IL-17 production by peripheral splenocytes was observed in response to MHC class II–restricted viral epitopes or UV-TMEV, but not MHC class I–restricted epitopes (Fig. 3 E). In contrast, levels of viral antigen–specific IFN-γ responses were similar in both the virus-infected PBS- and LPS-treated groups. Because it was previously reported that Th1 responses antagonize Th17 development (2, 4), finding similar levels of Th1 cells in both groups of TMEV-infected mice was unexpected. To further determine the role of IL-6 in the increased generation of Th17 cells in virus-infected mice, we compared levels of Th17 cells in virus-infected LPS-treated WT and IL-6 KO B6 mice (Fig. 3, F and G). Although similar levels of IFN-γ–producing CD4$^+$ T cells were observed in the CNS of virus-infected WT and IL-6 KO mice, the development of Th17 cells in the CNS was abrogated in IL-6 KO mice (Fig. 3 F). In addition, viral titers in the CNS of LPS-treated IL-6 KO mice were significantly lower at days 8 and 21 after TMEV infection compared with those of LPS-treated WT mice (Fig. 3 G). Collectively, these results clearly demonstrate that both viral persistence and the development of TMEV-induced demyelinating disease in LPS-treated B6 mice strongly correlate with elevated Th17 cell levels in the CNS in an IL-6–dependent manner.
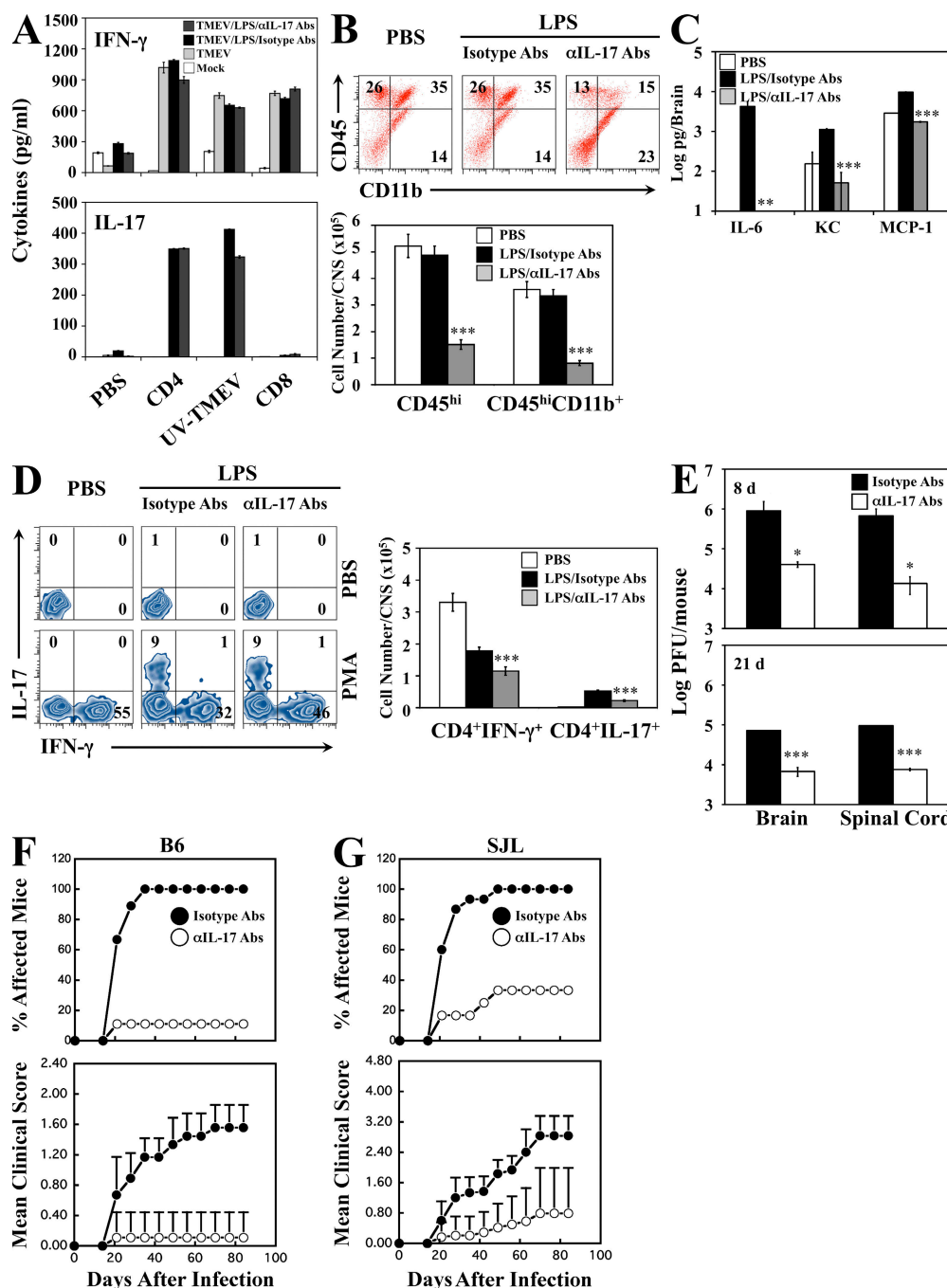
Treatment with antibodies to IL-17 inhibits viral persistence and disease development

Recent reports indicate that Th17 cells and their cytokine IL-17 play a pivotal role in tissue inflammation and damage, causing CNS demyelination in experimental autoimmune encephalomyelitis and perhaps also in human multiple sclerosis (4, 11). To determine whether this T cell type is also involved in the establishment of viral persistence and the consequent pathogenesis of chronic demyelinating disease, either neutralizing anti–IL-17 antibodies or isotype control antibodies were administered to LPS-treated B6 mice at days 0, 7, and 14 relative to TMEV infection (Fig. 4, A–F). Treatment with anti–IL-17 antibody reduced serum IL-17 to nearly undetectable levels during acute viral infection (8 d after infection) compared with treatment with isotype antibody, indicating the effectiveness of neutralizing antibodies (Fig. S3 A, available at http://www.jem.org/cgi/content/full/jem.20082030/DC1). Interestingly, IFN-γ and IL-17 levels produced by splenocytes in response to CD4 epitopes, UV-TMEV, and CD8 epitopes in the control group treated with isotype antibodies were comparable with mice treated with anti–IL-17 antibody (Fig. 4 A), suggesting that anti–IL-17 antibody treatment neutralizes IL-17 without eliminating Th17 cells. However, cellular infiltration (CD45^{hi} leukocytes and CD45^{hi}CD11b$^+$ macrophages) to the CNS was decreased by more than twofold at day 8 after infection. Levels of Th17-associated IL-6, KC, and MCP-1 were also lower in the CNS of anti–IL-17 antibody–treated mice than in isotype antibody–treated mice (Fig. 4, B and C). Despite low levels of leukocyte infiltration in anti–IL-17 antibody–treated mice, IFN-γ and IL-17 production by CD4$^+$ T cells (Fig. 4 D) and IFN-γ production by CD8$^+$ T cells (Fig. S3 B) in the CNS were uncompromised. We further analyzed whether TMEV persists and induces chronic demyelinating disease in these antibody-treated mice. Viral persistence in the CNS was significantly lower at days 8 and 21 after infection in the anti–IL-17–treated group versus the control antibody–treated group (Fig. 4 E and Fig. S4 C). Furthermore, drastic reductions (P < 0.01) in the incidence and severity of demyelinating disease were observed in the anti–IL-17–treated group compared with control groups of LPS-treated B6 (Fig. 4 F) and susceptible SJL mice (Fig. 4 G). Histological examinations of these anti–IL-17 antibody–treated groups displayed very little cellular infiltration and demyelination in spinal cords, in contrast to extensive demyelination and cellular infiltration in isotype control groups (Fig. S4, A and B). Thus, the elimination of IL-17 function from virus-infected mice appears to prevent the development of demyelinating disease. These results clearly indicate that IL-17 plays a critical pathogenic role in the establishment of viral persistence and pathogenesis of chronic demyelinating disease in both temporarily converted genetically resistant B6 mice that have become susceptible after LPS treatment (Fig. 4 F) and genetically susceptible SJL mice (Fig. 4 G).

IL-17 augments the production of virus-induced IL-6, KC, and MCP-1 in permissive cells and protects virus-infected cells from apoptosis

Because the above observations suggest that IL-17 plays an important role in promoting viral persistence and the consequent pathogenesis of inflammatory demyelinating disease (Fig. 4), we next determined whether or not IL-17 is able to directly enhance viral replication and inflammatory mediator production in permissive cells in vitro (Fig. 5). As expected, a marked reduction of TMEV infection/replication at 24 h after infection was observed in CD11c$^+$ BMDCs and primary astrocytes pretreated with IFN-γ (Fig. 5, A and C). However, viral infection/replication levels were similar in IL-17–pretreated and untreated cells (Fig. 5, A and C). Despite similar levels of viral replication in IL-17–pretreated and untreated cultures, the production of IL-6, KC, and MCP-1, but not IL-12p40, was markedly increased in both IL-17–treated DCs and astrocytes after TMEV infection as compared with control PBS-treated cultures (Fig. 5, B and D). Thus, these increases in cytokines and chemokines likely participate in further augmenting Th17 development and selective cellular infiltration in the virus target organ, as previously shown (10, 33). Furthermore, IL-17 treatment significantly inhibited virus-induced apoptosis of BM cells and primary astrocytes but not differentiated BMDCs (Fig. 5 E). Consequently, this IL-17–mediated protection against apoptosis likely promotes viral persistence in the CNS of virus-infected mice, as shown with an increase in virus yield by inhibiting

Figure 4. Treatment of mice with anti–IL-17 antibody inhibits viral persistence and the development of demyelinating disease. (A) Spleno-cytes from B6 mice treated with PBS alone, LPS and isotype control antibody (TMEV/LPS/Isotype Abs), or anti–IL-17 antibody (TMEV/LPS/αIL-17 Abs) 8 d after mock or TMEV infection were restimulated with mixed CD4 epitopes, UV-TMEV, or mixed CD8 epitopes. Cytokines produced in culture supernatants were analyzed using ELISA. (B) Flow cytometry of CNS-infiltrating cells from these mice at 8 d after infection (percentages are shown). The bar graph shows numbers of CNS-infiltrating CD45^{hi} leukocytes and CD45^{hi}CD11b$^+$ macrophages. ***, P < 0.001 for anti–IL-17 versus isotype antibody–treated groups. (C) Levels of IL-6, KC, and MCP-1 in the brains from TMEV-infected B6 mice. **, P < 0.01; and ***, P < 0.001 for anti–IL-17 versus isotype antibody groups. (D) Intracellular cytokine production by CNS-infiltrating cells after restimulation with PMA plus ionomycin. All flow plots display gated CD4$^+$ T cells (percentages are shown). The bar graph shows numbers of cytokine-secreting CD4$^+$ T cells. ***, P < 0.001 between groups treated with anti–IL-17 and isotype control antibodies. (E) Viral persistence levels in the CNS 8 and 21 d after infection were determined by plaque assay. *, P < 0.05; and ***, P < 0.001 between anti–IL-17 and isotype control groups. Data in A–E represent values from a single experiment conducted with pools of spleens or CNS of two mice per group (means ± SD are shown). Three independent experiments were performed to verify the results. (F and G) B6 mice treated with LPS (F) and SJL mice (G) were infected with TMEV in conjunction with isotype control (n = 9) or anti–IL-17 (n = 9) antibody treatment. The effects of anti–IL-17 anti-body treatment on disease development were confirmed once by separate experiments (means ± SD are shown).

apoptosis of virus–infected cells (34). The failure of IL-17 treatment to protect BMDCs from apoptosis was not caused by the lack of IL-17R expression (Fig. S5 A, available at http://www.jem.org/cgi/content/full/jem.20082030/DC1), suggesting the involvement of other factors in this protection. Interestingly, IL-17–mediated protection of BM cells appears to be restricted to certain inducers, as apoptosis induced by dexamethasone and anti-Fas mAb using the caspase 8 pathway, but not C2-ceramide and UV irradiation using alternative pathways, was inhibited (Fig. S5 B). Collectively, these findings indicate that IL-17 augments inflammatory responses by amplifying the production of proinflammatory cytokines and protecting virus-infected cells from apoptotic death.

IL-17 inhibits antiviral cytotoxic T cell function in vitro

The potential roles of Th17 cells and IL-17 on cytotoxic CD8+ T cell function are unknown. Because treatment of mice with anti–IL-17 antibodies enhances viral clearance from the CNS (Fig. 4), we explored the possibility that IL-17

compromises the cytotoxic function of CD8+ T cells, which are the key host defense immune mechanism against viral infections. Splenocytes from virus-infected B6 mice at the peak of acute infection were pretreated for 24 h or treated simultaneously with IL-17 and then assessed for cytolytic function with a typical short-term (6-h) cytotoxicity assay using VP2$_{121-130}$–loaded EL-4 target cells. Although the specific lytic activity of CD8+ T cells was slightly lower (not statistically significant) after pretreatment with IL-17 for 24 h, it remained unchanged after simultaneous treatment with IL-17 (Fig. 6 A). Similarly, IL-17 treatment did not significantly alter levels of granzyme B and IFN-γ on CD8+ T cells (Fig. 6 B). In contrast, IL-17, but not IL-17F, which has a high degree of homology with IL-17 (35), abrogated the slow (60-h) lytic reaction (Fig. 6 C) that is prominently mediated by the Fas–FasL pathway (36). This lytic reaction was similarly inhibited with IL-17 pretreatment of target cells but not effector cells (Fig. 6 C), indicating that IL-17 treatment impedes cytolytic function of CD8+ T cells through signaling on target cells.
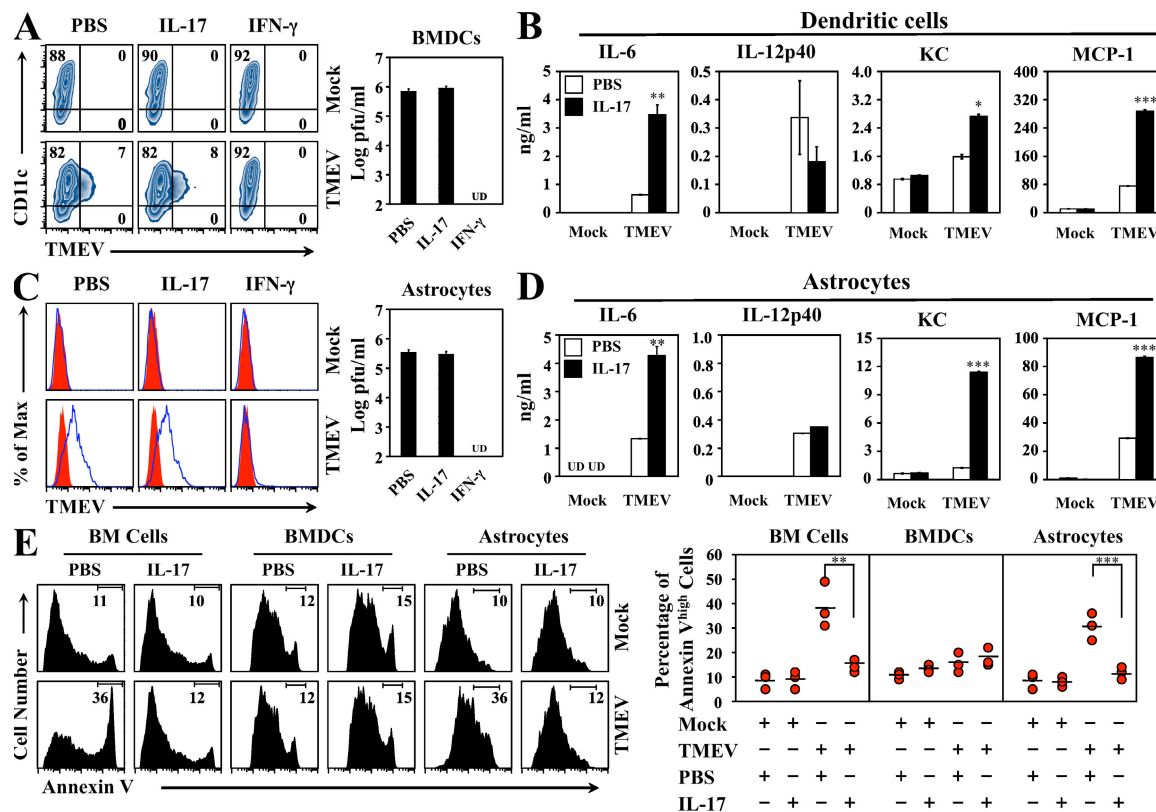
Figure 5. IL-17 enhances virus–induced production of inflammatory cytokines and protects against infection–induced cell apoptosis.
(A–D) B6 BMDCs (A) and astrocytes (C) pretreated with IL-17 or IFN-γ for 6 h were infected with TMEV for 24 h. Levels of viral infection were assessed using flow cytometry after staining with anti-TMEV antibody or plaque assay with culture supernatants of TMEV-infected cells. The numbers in each quadrant represent percentages. UD, undetectable values <100 PFU/ml. (C) Histograms represent astrocytes stained with isotype control (red) and anti-TMEV antibody (open). Cytokine levels in B6 BMDCs (B) and astrocytes (D) infected with TMEV for 24 h in the presence of PBS or IL-17 were measured using ELISA. UD, undetectable values <10 pg/ml. *, P < 0.05; **, P < 0.01; and ***, P < 0.001 for IL-17– versus PBS-treated cultures. Data in A–D are representative of four separate experiments (means ± SD are shown). (E) TMEV infection–induced cell apoptosis was determined using flow cytometry of BM cells (2-d culture), BMDCs (5-d culture), and neonatal astrocytes 24 h after coincubation with PBS or IL-17. The number in each histogram represents the percentage of Annexin V^{high} cells. The graph shows data from three independent experiments. The horizontal bar represents the mean of the group. **, P < 0.01; and ***, P < 0.001 between IL-17– versus PBS-treated cultures.

320

IL-17 PROMOTES VIRAL PERSISTENCE AND PATHOGENESIS | Hou et al.

To determine whether IL-17 inhibits cytotoxic function by blocking apoptosis of target cells during long-term cytolytic reactions, levels of apoptotic cells were analyzed (Fig. 6 D). The results showed that target cells are completely protected from CD8+ T cell–mediated apoptosis in the presence of IL-17, whereas effector CD8+ T cells remain unaltered. We further assessed the effects of an inhibitor of Fas–FasL interaction using human Fas:Fc (Fas–IgG Fc fusion protein) on IL-17–mediated inhibition of cytotoxic function to confirm the involvement of the Fas-dependent pathway (Fig. 6 E). The addition of Fas:Fc protein dramatically inhibited slow CD8+ T cell–mediated lysis in the absence of IL-17 but not in the presence of IL-17, strongly suggesting that IL-17 interferes with CD8+ T cell cytotoxic function via blocking the Fas–FasL pathway (Fig. 6 E), consistent with the inhibition of anti-Fas antibody–induced apoptosis by IL-17 (Fig. S5).

We further examined whether IL-17 exerts a similar effect on CD4+ T cell–mediated apoptosis, because MHC class II–restricted CD4+ T cell–mediated killing of target cells during viral infection has been reported (37, 38). We used the OT-II TCR transgenic system to address the effects of IL-17 treatment on CD4+ T cell–mediated killing of epitope peptide–loaded target B cells. Again, the presence of IL-17 significantly (greater than twofold) inhibited the apoptosis of OVA$_{323-339}$–loaded B cells induced by cognate interactions with OT-II CD4+ T cells (Fig. 6 F). To further understand the underlying mechanisms for protection of immune target cells by IL-17, expression levels of prosurvival B cell lymphoma–xl (Bcl-xl) and Bcl-2 proteins in B cells, BM cells, and BMDCs were assessed after treatment with IL-17 (Fig. 6 G). B cells and BM cells, but not BMDCs, displayed elevated expression of both Bcl-xl and Bcl-2 in response to IL-17 treatment (Fig. 6 G), suggesting that IL-17–induced up-regulation of prosurvival protein expression contributes to the protection of target cells from effector T cell–mediated killing. Thus, IL-17 apparently inhibits antiviral cytotoxic T cell function in vitro by protecting target cells from effector T cell–induced apoptosis.

### Anti–IL-17 antibody–treated mice display enhanced antiviral cytotoxic T cell function in vivo

To correlate the above in vitro results of enhanced target cell survival by IL-17 treatment (Fig. 6) with those in virus-infected mice in vivo, we sought to examine whether administration of anti–IL-17 antibody into virus-infected SJL mice reduces the number of virus-permissive cells in the target organ (CNS) and enhances antiviral cytotoxic T cell function. 8 d after infection, the proportion and number of CNS-infiltrating macrophages were significantly lower in anti–IL-17 antibody–treated mice than in isotype antibody–treated mice (Fig. 7 A), suggesting that cellular infiltration is affected by antibody treatment, as previously reported (5). In contrast, a similar proportion and number of CNS-resident microglia were observed in both anti–IL-17 and isotype antibody–treated mice (Fig. 7 A). Notably, the expression of prosurvival Bcl-xl and Bcl-2 proteins in both infiltrating macrophages

and resident microglia was reduced in anti–IL-17 antibody–treated mice compared with isotype antibody–treated mice (Fig. 7 B). This reduction of antiapoptotic proteins was not detectable in antiviral effector CD4+ and CD8+ T cells (Fig. 7 C). These results indicate that virus-permissive cells from anti–IL-17 antibody–treated mice became more susceptible to apoptosis. If this is the case, anti–IL-17 antibody–treated mice would be expected to develop low numbers of virus-specific CD8+ T cells corresponding to their limited viral load. To examine this possibility, levels of virus-specific CD8+ T cells were assessed using intracellular IFN-γ staining after in vitro restimulation with dominant and subdominant VP3 epitopes (Fig. 7 D). The results indicate that the proportion of virus-specific CD8+ T cells in the CNS of anti–IL-17 antibody–treated mice is higher yet the overall number is lower compared with isotype-treated mice. To further analyze antiviral cytotoxic T cell function in antibody-treated mice, in vivo lytic responses to target cells loaded with dominant and subdominant viral epitopes were investigated (Fig. 7 E). TMEV-infected susceptible mice treated with anti–IL-17 antibody displayed significantly increased elimination of newly introduced viral epitope peptide–loaded target cells. Collectively, these results clearly indicate that anti–IL-17 antibody treatment enhances the function of antiviral cytotoxic T cells by facilitating the removal of virus-infected target cells during viral infection, leading to efficient viral clearance and, consequently, reduced disease development.

DISCUSSION

We have presented evidence in this paper that virus-infected DCs polarize the development of CD4+ T cells toward the Th17 type. During acute viral infection, Th17 cytokine IL-17 promotes virus-induced inflammatory mediators in permissive cells to form a pathogenic inflammatory milieu, as well as to protect cells from both virus- and effector T cell–induced apoptosis, resulting in chronic viral persistence and demyelinating disease. By interfering with cytolytic T cell function, IL-17 blocks vigorous and efficient antiviral immunity, thereby permitting sustained viral infection. This IL-17–mediated feedback loop during viral infection favors viral escape from powerful antiviral effector T cells. These properties of Th17 cells represent a previously unknown mechanism of viral persistence leading to the pathogenesis of virus-induced chronic diseases.

Our data show that TMEV-infected DCs promote the development of Th17 cells in vitro (Fig. 1). These results strongly suggest that virus infection harnesses the ability of DCs to polarize CD4+ T cells toward Th17 cells. In particular, IL-6 produced by DCs after viral infection appears to steer this skewed Th17 cell development. It is interesting to note that higher levels of Th17 cells are found in TMEV-infected SJL mice than in B6 mice (Fig. 2). This difference between resistant B6 and susceptible SJL mice may reflect the differential level of Th17 cell generation induced by DCs (Fig. 1, A vs. E; and Fig. S2). LPS treatment likely enhances virus-infected DCs to induce Th17 development to the
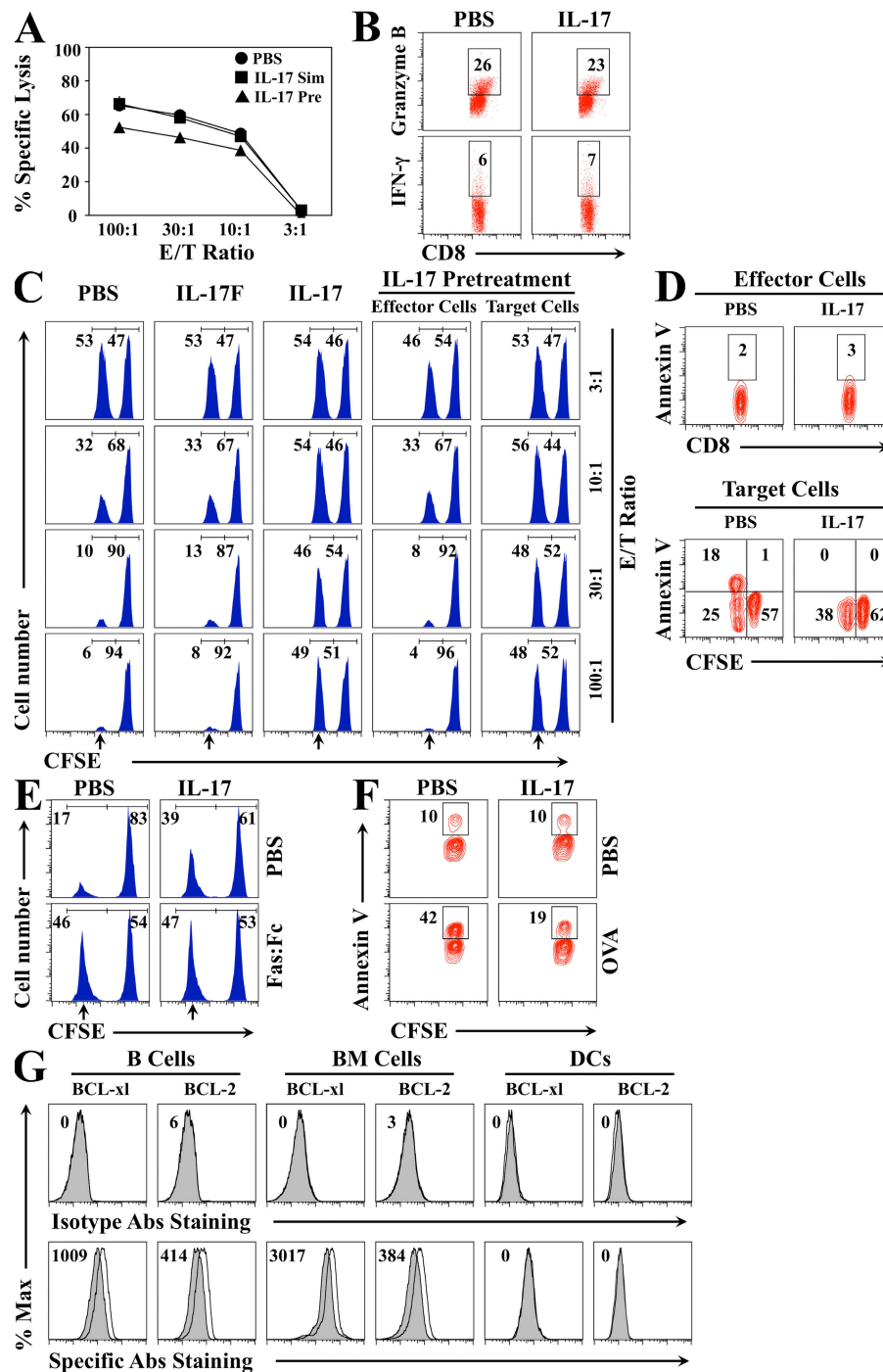
Figure 6. IL–17 inhibits antiviral cytotoxic T cell function. (A) Splenocytes from B6 mice at 8 d after infection were pretreated for 24 h or were simultaneously treated with IL-17 (IL-17 Pre or IL-17 Sim, respectively), and were then subjected to a ^{51}Cr-release assay using VP2$_{121-130}$–loaded EL-4 target cells. (B) Splenocytes (effector cells) from TMEV-infected B6 mice were co-cultured with naive B6 splenocytes (target cells) loaded with VP2$_{121-130}$ for 24 h in the presence of IL-17 at an E/T ratio of 10:1. The numbers in the plots indicate the frequency of granzyme B– or IFN-γ–positive CD8+ T cells. (C) Splenocytes from naive B6 mice were loaded with VP2$_{121-130}$ or OVA$_{323-339}$ peptides and labeled with a lower or higher concentration of CFSE, respectively, as target cells. The labeled target and effector cells were pretreated separately with IL-17 for 24 h and co-cultured or cultured together in the presence of IL-17F or IL-17 for an additional 60 h. The numbers in each histogram represent percentages of the lower (VP2$_{121-130}$) and higher (OVA$_{323-339}$) concentrations of CFSE-labeled cells. The arrow shows the specific killing of target cells. (D) Apoptosis levels of effector and target cells from the cultures in C at an E/T ratio of 10:1 were assessed after a 24-h incubation (percentages are shown). (E) Levels of target cell destruction in the presence of Fas:Fc were assessed 60 h after co-culture with effector cells at an E/T ratio of 30:1 (percentages are shown). The arrows show virus-specific killing. (F) Levels of antigen-loaded B cell killing by activated CD4+ T cells were determined. Peptide-loaded B cells were co-cultured in the presence of LPS and PBS or IL-17 at a

pathogenic threshold of Th17 response in resistant B6 mice (Fig. 3), as shown in vitro (Fig. S2). This difference in Th17 cell levels in the CNS of virus-infected mice correlates with IL-6 levels produced both in the CNS of TMEV-infected mice (39) and by in vitro–infected antigen-presenting cells, including DCs and microglia from susceptible SJL versus resistant B6 mice (30, 40). An elevated level of IL-6 appears to be necessary for this skewing of Th17 cell differentiation by virus-infected DCs in vitro (Fig. 1), as well as in virus-infected mice (Fig. 3). It is conceivable that the cellular sources of IL-6 during virus infection may also include many different CNS-resident cells such as microglia and astrocytes, which serve as major potential viral reservoirs, and infiltrating cells, including DCs and macrophages (30, 40–42). Moreover, preferential expression of TGF-β was found in the CNS of TMEV-infected SJL mice but not in B6 mice (39), suggesting that TGF-β may also participate in the development of Th17 cells in the CNS, because the differentiation of Th17 cells requires TGF-β (6–8). Thus, innate inflammatory responses to TMEV infection in DCs and other antigen-presenting cells would most likely affect the development of Th17 cells, leading to a critical modulation of adaptive immune responses involved in virus–host interactions.

In contrast to resistant B6 mice that display rapid viral clearance and the absence of demyelinating disease development after TMEV infection, susceptible SJL mice exhibit chronic viral persistence and disease progression (28, 29). Active viral replication is a critical determinant for persistent infection and the development of chronic demyelinating disease (43). In addition, virally induced inflammatory mediators may also contribute to this harmful process. Although IL-17 does not directly enhance TMEV infection/replication in permissive cells, this cytokine significantly increases the production of virus-induced inflammatory mediators such as IL-6, KC, and MCP-1 (Fig. 5). This suggests that IL-17–mediated signals amplify virus-induced innate responses involved in CNS inflammation, which leads to chronic demyelination. Consistent with our findings, a recent report indicated that IL-17 synergistically enhances human rhinovirus-16–induced epithelial production of the inflammatory mediator IL-8, a human homologue for mouse KC protein (44).

Previously, the pathogenic role of CD4+ T cells had been proposed based on delayed disease development after treatment with anti–MHC class II antibody (28, 29). The protective role of CD4+ T cells has also been noted, as virus-infected CD4 or MHC class II KO mice succumb to TMEV-induced demyelinating diseases. However, these studies are difficult to interpret partly because of the lack of protective Th1 as well as reduced CD8+ T cells in the absence of CD4+ T cell help. It is interesting to note that immunization with CD4 epitope

before viral infection protects mice from disease development, whereas such immunization after viral infection exacerbates disease progression, suggesting that expansion of CD4+ T cells after infection may be pathogenic (45). Although the protective roles of Th1 and its hallmark cytokine, IFN-γ, have been previously documented, the roles of Th17 and IL-17 in viral infection–induced inflammatory disease remain undefined. This cell linage plays a critical role in the protection against extracellular bacterial or fungal infections (2, 5–9). In contrast, virus-specific Th17 cells are detectable during early HIV infection (17), suggesting that Th17 cells may be associated with viral replication. Interestingly, mice lacking both of the transcription factors T-bet and eomesodermin develop high levels of IL-17–producing CD8+ T cells; these mice develop a progressive inflammatory and wasting syndrome after lymphocytic choriomeningitis viral infection (25). Our results clearly demonstrate that Th17 cells and their cytokine IL-17 play a critical role in the pathogenesis of TMEV-induced chronic demyelinating disease (Fig. 4), similar to that shown with experimental autoimmune encephalomyelitis and perhaps also human multiple sclerosis (4, 11). Therefore, it is most likely that the pathogenic function of infection-induced Th17 cells observed with the TMEV model system is also applicable to other persistent viral infections, although this has yet to be determined. Furthermore, our data indicate that the pathogenic role of Th17 cells is not mouse strain specific. Both genetically resistant B6 mice in conjunction with LPS treatment and susceptible SJL mice induce elevated Th17 responses and chronic viral infection leading to the development of demyelinating disease (Figs. 3 and 4). In particular, demyelinating disease development in genetically resistant B6 mice in conjunction with LPS treatment suggests that a cytokine milieu induced by opportunistic infections of bacterial agents promotes Th17 responses during viral infection, leading to viral persistence and chronic infection–associated diseases. Such an enhanced development of pathogenic Th17 responses may result in clinical episodes in which the timing of infection strongly coincides with the exacerbation of severe clinical symptoms in human multiple sclerosis, as well as in acute disseminated encephalomyelitis (46–49).

One intriguing finding in this study is that IL-17 impairs antiviral cytotoxic CD8+ T cell responses (Figs. 6 and 7). This regulatory role of IL-17 on CD8+ T cell function had not previously been identified. In our system, TMEV infection in susceptible mice promotes the generation of Th17 cells that compromise antiviral cytotoxic T cell function via IL-17 production. Previous findings that IL-17 promotes tumor growth (50, 51) may also reflect the inhibitory effect of IL-17 on cytotoxic CD8+ T function against target tumor cells. It is well established that cytotoxic CD8+ T cells confer protective

---

1:5 ratio for 24 h with effector OT-II T cells that were preactivated with anti-CD3/CD28 antibodies. The numbers in each plot indicate the frequency of Annexin V+ B220+ B cells. (G) Intracellular expression levels of Bcl-xl and Bcl-2 proteins in LPS-stimulated B cells, BM cells, and BMDCs from naive B6 mice were assessed after a 24-h incubation with PBS (shaded histogram) or IL-17 (open histogram). Relative median fluorescence intensity differences between the IL-17 and the PBS group are illustrated on the flow histograms. Data are representative of four independent experiments.

immunity to viral infection (52) by secreting antiviral cytokines or inducing the cytolysis of infected cells via the granule exocytosis and/or Fas–FasL pathway (53–55). In addition, similar cytolysis of virus-infected cells is observed by CD4^{+} T cells in an MHC class II–restricted manner during virus infection (37, 38, 56). Our results indicate that IL-17 interferes with the Fas–FasL pathway of cytotoxic effector CD4^{+} and CD8^{+} T cells by protecting target cells against apoptosis, pos-

sibly through the up-regulation of their prosurvival proteins (Fig. 6). Because an IL-17 receptor–like gene has recently been identified as a novel antiapoptotic gene (57), it is conceivable that the IL-17 receptor may have such an antiapoptotic property. Furthermore, Th17 cytokines other than IL-17 may be able to modulate protective antiviral T cell responses. For example, IL-21, an essential cytokine for the induction and maintenance of Th17 cells, has the potential to suppress the
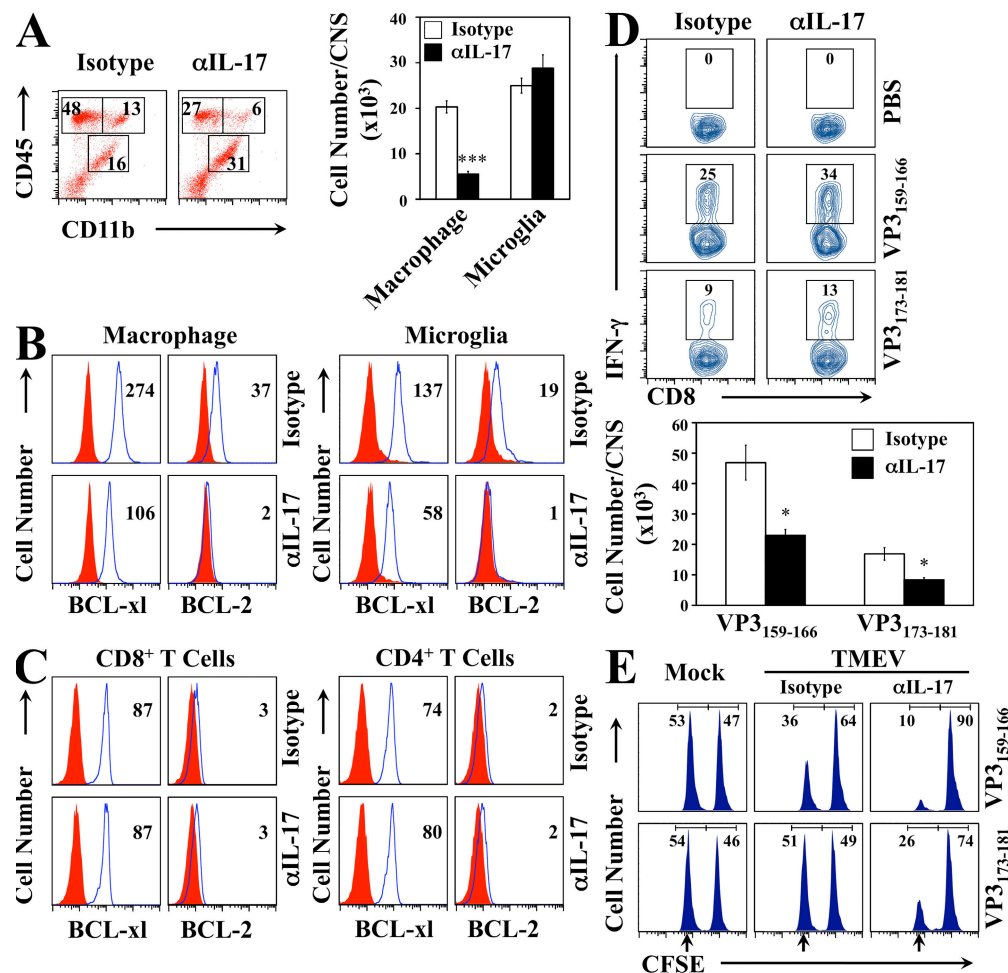
Figure 7. Treatment of virus–infected mice with anti–IL-17 antibody elevates antiviral cytotoxic T cell function. (A) Flow cytometry of CNS-infiltrating cells from SJL mice treated with isotype or anti–IL-17 antibody at 8 d after infection (percentages are shown). The bar graph represents numbers of CNS-infiltrating CD45^{hi}CD11b^{+} macrophages and resident CD45^{int}CD11b^{+} microglia. ***, P < 0.001 for anti–IL-17 versus isotype antibody–treated groups. (B and C) Intracellular expression of Bcl-xl and Bcl-2 in CNS macrophages and microglia (B) and CNS-infiltrating CD4^{+} and CD8^{+} T cells (C) isolated from SJL mice treated with isotype or anti–IL-17 antibody. Shaded and open histograms represent cells stained with isotype control and anti-Bcl antibodies, respectively. The number in each histogram shows the relative median fluorescence intensity difference between cells stained with anti-Bcl antibody and isotope control antibody. (D) Intracellular cytokine production by CNS-infiltrating cells from isotype or anti–IL-17 antibody–treated SJL mice was determined. The number in each plot indicates the frequency of IFN-γ–producing CD8^{+} T cells. The bar graph represents numbers of IFN-γ–producing viral epitope-specific CD8^{+} T cells. *, P < 0.05, anti–IL-17 versus isotype antibody–treated groups. Data in A–D represent pooled CNS cells from three mice per group and are representative samples of three separate experiments (means ± SD are shown in A and D). (E) Enhanced lysis of dominant epitope VP3[159–166]– and subdominant epitope VP3[173–181]–loaded target cells in TMEV-infected SJL mice treated with anti–IL-17 antibody. SJL mice were treated with either isotype (n = 3) or anti–IL-17 (n = 3) antibody at days 0 and 7 relative to TMEV infection. At 8 d after infection, in vivo lysis activity was evaluated in virus- and mock-infected mice (n = 3) that received the target cell injection. The numbers in each histogram show the percentages of CFSE-labeled virus epitope–loaded (lower fluorescence intensity) and OVA[323–339]–loaded (higher fluorescence intensity) target cells, respectively. The arrows represent the virus epitope–loaded target cells. One representative mouse from three mice per group is shown. The pattern of every mouse in each group was very consistent. These experiments were repeated once with three additional mice.

production of IFN-γ by T lymphocytes and to drive cytotoxic CD8+ T cells to apoptosis (58–61). In addition, a TMEV susceptibility locus, *Tmevp3*, coincides with the IL-22 gene, which encodes IL-22, a Th17 cytokine (62), suggesting a potential role of this T cell population in the development of demyelinating disease. More studies with these cytokines would be helpful in clarifying the role of Th17 cells in the establishment of viral persistence and the consequent pathogenesis of virus-induced chronic inflammatory diseases.

In summary, viral infection in antigen-presenting cells in vitro as well as in susceptible mice in vivo induces elevated IL-6 production that subsequently promotes the development of pathogenic Th17 cells. Th17 cells and their cytokine IL-17 are potent promoters of viral persistence and the development of virally induced chronic inflammatory demyelinating disease. IL-17 inhibits virus–induced cell apoptosis; this protection of virus–infected cells serves as a powerful means for viral evasion of the immune system. The inhibition of apoptosis prolongs the life of infected cells on the one hand, and desensitizes killing by cytotoxic T cells on the other, resulting in enhanced viral replication and persistence. The virus–host interaction via Th17 cells and/or their cytokine IL-17 results in the establishment of persistent viral infection and harmful immune responses, leading to the pathogenesis of TMEV-induced demyelinating disease. Conversely, interference with this interaction by neutralizing IL-17 activity reduces lymphocyte infiltration to the CNS and inhibits disease development. This particular interaction may also potentially operate in other chronic diseases associated with a variety of viral infections and could be a target for therapeutic intervention.

MATERIALS AND METHODS

Mice. Female SJL/J (SJL) and C57BL/6 (B6) mice were purchased from Harlan Sprague Dawley. IL-6 KO (IL-6$^{-/-}$) mice on a B6 background were obtained from the Jackson Laboratory. 6–8-wk-old mice were maintained and used according to the protocols approved by the Northwestern University Animal Care and Use Committee. TCR transgenic mice that recognize TMEV capsid protein peptide VP2$_{74-86}$ were generated with the genomic DNA of a T cell clone derived from the spinal cords of TMEV-infected SJL mice (63) by the Transgenic Core Facility at Northwestern University. Transgenic founder mice were backcrossed to SJL mice at least 14 generations.

TMEV-induced demyelinating diseases. Mice were intracerebrally infected with 30 μl (10^6 PFU) of the BeAn strain of TMEV, and clinical symptoms of disease were assessed weekly, as previously described (30). For LPS treatment, B6 or IL-6 KO mice were intraperitoneally injected with LPS (20 μg/100 μl per mouse; *Escherichia coli* 0111:B4; Sigma-Aldrich) at days 0 and 5 relative to viral infection. For neutralization of IL-17 in vivo, mice were intraperitoneally injected with 100 μg anti–mouse IL-17A antibody (clone eBioMM17F3; eBioscience) in 200 μl at days 0, 7, and 14 relative to viral infection.

BMDCs, primary astrocyte cultures, and viral infection/replication assay. BMDCs were generated in the presence of GM-CSF for 5 d, as previously described (30, 64). Primary astrocytes were generated from 1–3-d-old B6 neonates by differential shaking, as previously described (42). Virus infection/replication assays were performed 24 h after viral infection, as previously described (30). Cells were subsequently fixed, permeabilized (perm/fix solution; BD), blocked with 1% normal goat serum (Invitrogen), and stained with mouse anti–TMEV 8C mAb (65) followed by FITC-conjugated goat anti–mouse secondary antibody (Invitrogen). BMDCs were further stained with anti-CD11c–allophycocyanin (APC; BD). Levels of infectious virus in culture supernatants were determined with a standard plaque assay, as previously described (30). The cytokines in culture supernatants were analyzed using ELISA kits for IL-6, IL-12p40, IL-12p70, and MCP-1 (OptEIA; BD); for IL-23 (eBioscience); and for KC (R&D Systems). For the cell death assay, adult B6 BM cells from a 2-d culture with GM-CSF, BMDCs from a 5-d culture, and neonatal astrocytes were infected for 24 h with TMEV (multiplicity of infection [MOI] of 10) in the presence or absence of 100 ng/ml IL-17 (PeproTech), and were then stained with APC-conjugated Annexin V (Invitrogen).

Isolation of CNS-infiltrated leukocytes and assessment of virus antigen-specific responses. CNS-infiltrating leukocytes were isolated from TMEV-infected mice, as previously described (30). Isolated CNS-infiltrating leukocytes were restimulated with different doses of UV-TMEV for 48 h. Splenocytes from virus-infected mice were cultured in the presence of 1 μg/ml UV-TMEV, 2 μM of mixed CD4 epitopes (VP4$_{25-38}$ and VP2$_{206-220}$), and 2 μM of mixed CD8 epitopes (VP2$_{121-130}$, VP3$_{110-120}$, and VP2$_{165-173}$), as previously described (66). All peptides were synthesized by GeneMed Synthesis Inc. and used as previously described (67). IFN-γ and IL-17 levels in culture supernatants were assessed using ELISA kits (from BD [OptEIA] and R&D Systems, respectively).

Measurement of viral persistence in the CNS. Brains and spinal cords were isolated from TMEV-infected mice after cardiac perfusion with Hank's buffered salt solution. A standard plaque assay was performed using tissue homogenates, as previously described (30).

Intracellular staining and flow cytometry. For assessment of cytokine production by OT-II transgenic T cells, CD4+ T cells were isolated from OT-II mice by positive immunomagnetic cell sorting (Miltenyi Biotec), primed with mock or TMEV-infected B6 BMDCs in the presence of OVA$_{323-339}$ for 4 d with or without IL-6 (both from PeproTech), or anti–mouse IL-6 antibody (Invitrogen). These cultures were restimulated with 50 ng/ml PMA and 1 μg/ml ionomycin (Sigma-Aldrich) for 6 h and were stained with anti–IFN-γ–APC, anti–IL-17–PE, and anti-CD4–FITC (all from BD). In some experiments, BMDCs were left unfixed or fixed with 0.1% paraformaldehyde, as previously described (30). To determine the level of IL-17 production by the whole CNS cells, CNS-infiltrating leukocytes from TMEV-infected SJL and B6 mice at 8 d after infection were cultured with PMA plus ionomycin for 6 h and analyzed by flow cytometry. Levels of virus-specific CNS-infiltrating CD8+ T cells were assessed by flow cytometry after intracellular staining of IFN-γ after stimulating CNS mononuclear cells for 6 h with dominant epitope VP3$_{159-166}$ or subdominant epitope VP3$_{173-181}$. All antibodies used in flow cytometry for cellular markers were purchased from BD. To analyze the expression of prosurvival proteins, splenic B cells were isolated by using anti-CD19 MicroBeads (Miltenyi Biotec). B cells stimulated with 10 μg/ml LPS, BM cells, and BMDCs were treated for 24 h with or without 100 ng/ml IL-17. These cells were then stained with anti–mouse Bcl-xl–FITC (Santa Cruz Biotechnology, Inc.) or anti–mouse Bcl-2–FITC (eBioscience) and analyzed using flow cytometry. To determine expression levels of prosurvival proteins in vivo, CNS-infiltrating cells were isolated from TMEV-infected SJL mice treated with anti–IL-17 antibody at days 0 and 7 relative to viral infection. These cells were stained with anti–mouse CD45-APC and anti–mouse CD11b-PE (both from BD) for antigen-presenting cells, and anti–mouse CD4-APC or anti–mouse CD8-APC for T cells. All cells were further stained with anti–mouse Bcl-xl–FITC or anti–mouse Bcl-2–FITC and analyzed using flow cytometry.

Cytokine production assays. To assess cytokine production by VP2-TCR transgenic T cells, naive CD4+ T cells (CD4+CD25−CD44^{low}) sorted using a MoFlo (Dako) were co-cultured for 4 d with BMDCs pulsed with

PBS, 2 μM VP2$_{74-86}$, or 1 μg/ml UV–TMEV, or were infected with TMEV overnight. IL-17, IL-22, and TNF-α levels in culture supernatants were assessed using ELISA kits (from R&D System, Antigenix America Inc., and BD [OptEIA], respectively).

Quantitative analysis of mRNAs. Total RNA was extracted with TRIzol (Invitrogen) from CD4$^+$CD8$^-$, CD4$^-$CD8$^+$, and CD4$^-$CD8$^-$ mononuclear cells in the CNS of SJL and B6 mice by sorting on a MoFlo cytometer at 8 d after TMEV infection. Reverse transcription was performed using 1–3 μg of total RNA. The sense and antisense primer sequences for IL-17, RORγt, and GADPH were synthesized as previously described (29, 68). Specific RNA messages were amplified in SYBR green I mastermix (Bio-Rad Laboratories) by real-time PCR using an iCycler (Bio-Rad Laboratories). Expression levels of IL-17 and RORγt mRNAs were determined by comparison to GADPH expression. All real-time RCR was performed in triplicate.

Cytotoxic activity assay. VP2$_{121-130}$–loaded EL-4 cells were used as target cells for a standard ^{51}Cr-release assay to assess the short-term cytoxicity by virus-specific CD8$^+$ T cells, which were isolated from the spleen of B6 mice 8 d after TMEV infection, as previously described (67). For the long-term cytoxicity assay, aliquots of naive B6 splenocytes were pulsed with cognate peptide (VP2$_{121-130}$) or irrelevant peptide (OVA$_{323-339}$), and further labeled with low or high concentrations of CSFE, respectively. These labeled target cells were then co-cultured for 60 h with effector splenocytes from B6 mice at 8 d after TMEV infection at different effector/target (E/T) ratios in the presence or absence of 100 ng/ml IL-17F or IL-17 (PeproTech). In parallel experiments, labeled target and effector cells were pretreated separately with IL-17 for 24 h, and were then washed and co-cultured for 60 h. In some experiments, 1 μg/ml of recombinant human Fas:Fc and 1 μg/ml enhancer for receptors (both from Enzo Biochem, Inc.) were added to co-cultures to inhibit the Fas–FasL pathway. For apoptosis assays of effector and target cells, cells from the co-cultures at an E/T ratio of 10:1 for 24 h were stained with anti-CD8–PE (BD) and APC-conjugated Annexin V. The activated CD4$^+$ T cell–mediated cognate cytolysis of target B cells was analyzed as previously described (69). In brief, B cells purified from naive B6 mice by positive immunomagnetic cell sorting (Miltenyi Biotec) were stimulated with 10 μg/ml LPS for 20 h and pulsed with 100 μg/ml OVA for the final 2 h, and then cultured for 24 h at an E/T ratio of 5:1 with CD4$^+$ T cells from OT-II mice preactivated for 4 d with anti-CD3 plus anti-CD28 mAbs (both BD) in the presence of 0.5 μg/ml LPS. Cells were stained with anti-CD45R/B220–PE (BD) and APC-conjugated Annexin V. For in vivo cytolysis assays, aliquots of naive SJL splenocytes were pulsed with viral epitope peptide (VP3$_{159-166}$ or VP3$_{173-181}$) or irrelevant peptide (OVA$_{323-339}$), and respectively labeled with low or high concentrations of CSFE. The mixture of these two populations in equal numbers (10^7 total cells per mouse) was intravenously injected into mock or TMEV-infected SJL mice. After 15–18 h, splenocytes were isolated from recipients, and the relative numbers of each CFSE-stained population were assessed by flow cytometry.

Statistical analysis. The results were expressed as the mean ± SD, where applicable. The unpaired Student's *t* test was used to compare the two independent groups. Differences in mean incidence and severity score between the two experimental groups were compared between 21 and 84 d after infection by using the paired Student's *t* test. P < 0.05 was considered to be significant.

Online supplemental material. Fig. S1 shows the enhanced Th17 development during persistent viral infection. Fig. S2 demonstrates the elevated differentiation of Th17 cells induced by virus-infected DCs in the presence of LPS. Fig. S3 shows the cytokine production by CNS-infiltrating CD8$^+$ T cells after TMEV infection in B6 mice treated with anti–IL-17 antibodies. Fig. S4 compares the histopathology and viral persistence levels between mice treated with anti–IL-17 and control antibodies. Fig. S5 presents the expression of IL-17R on BM cells and the range of IL-17–induced protection against apoptosis triggered by various treatments. Online supplemental material is available at http://www.jem.org/cgi/content/full/jem.20082030/DC1.

REFERENCES

1. Abbas, A.K., K.M. Murphy, and A. Sher. 1996. Functional diversity of helper T lymphocytes. *Nature*. 383:787–793.

2. Harrington, L.E., R.D. Hatton, P.R. Mangan, H. Turner, T.L. Murphy, K.M. Murphy, and C.T. Weaver. 2005. Interleukin 17-producing CD4+ effector T cells develop via a lineage distinct from the T helper type 1 and 2 lineages. *Nat. Immunol.* 6:1123–1132.

3. Weaver, C.T., L.E. Harrington, P.R. Mangan, M. Gavrieli, and K.M. Murphy. 2006. Th17: an effector CD4 T cell lineage with regulatory T cell ties. *Immunity.* 24:677–688.

4. Steinman, L. 2007. A brief history of T(H)17, the first major revision in the T(H)1/T(H)2 hypothesis of T cell-mediated tissue damage. *Nat. Med.* 13:139–145.

5. Park, H., Z. Li, X.O. Yang, S.H. Chang, R. Nurieva, Y.H. Wang, Y. Wang, L. Hood, Z. Zhu, Q. Tian, and C. Dong. 2005. A distinct lineage of CD4 T cells regulates tissue inflammation by producing interleukin 17. *Nat. Immunol.* 6:1133–1141.

6. Veldhoen, M., R.J. Hocking, C.J. Atkins, R.M. Locksley, and B. Stockinger. 2006. TGFbeta in the context of an inflammatory cytokine milieu supports de novo differentiation of IL-17-producing T cells. *Immunity.* 24:179–189.

7. Bettelli, E., Y. Carrier, W. Gao, T. Korn, T.B. Strom, M. Oukka, H.L. Weiner, and V.K. Kuchroo. 2006. Reciprocal developmental pathways for the generation of pathogenic effector TH17 and regulatory T cells. *Nature.* 441:235–238.

8. Mangan, P.R., L.E. Harrington, D.B. O'Quinn, W.S. Helms, D.C. Bullard, C.O. Elson, R.D. Hatton, S.M. Wahl, T.R. Schoeb, and C.T. Weaver. 2006. Transforming growth factor-beta induces development of the T(H)17 lineage. *Nature.* 441:231–234.

9. McGeachy, M.J., and D.J. Cua. 2008. Th17 cell differentiation: the long and winding road. *Immunity.* 28:445–453.

10. Ouyang, W., J.K. Kolls, and Y. Zheng. 2008. The biological functions of T helper 17 cell effector cytokines in inflammation. *Immunity.* 28:454–467.

11. Bettelli, E., M. Oukka, and V.K. Kuchroo. 2007. T(H)-17 cells in the circle of immunity and autoimmunity. *Nat. Immunol.* 8:345–350.

12. Dong, C. 2008. TH17 cells in development: an updated view of their molecular identity and genetic programming. *Nat. Rev. Immunol.* 8:337–348.

13. Bettelli, E., T. Korn, M. Oukka, and V.K. Kuchroo. 2008. Induction and effector functions of T(H)17 cells. *Nature.* 453:1051–1057.

14. Maek-A-Nantawat, W., S. Buranapraditkun, J. Klaewsongkram, and K. Ruxrungtham. 2007. Increased interleukin-17 production both in helper T cell subset Th17 and CD4-negative T cells in human immunodeficiency virus infection. *Viral Immunol.* 20:66–75.

15. Ndhlovu, L.C., J.M. Chapman, A.R. Jha, J.E. Snyder-Cappione, M. Pagan, F.E. Leal, B.S. Boland, P.J. Norris, M.G. Rosenberg, and D.F. Nixon. 2008. Suppression of HIV-1 plasma viral load below detection preserves IL-17 producing T cells in HIV-1 infection. *AIDS.* 22:990–992.

16. Alfano, M., A. Crotti, E. Vicenzi, and G. Poli. 2008. New players in cytokine control of HIV infection. *Curr. HIV/AIDS Res.* 5:27–32.

17. Yue, F.Y., A. Merchant, C.M. Kovacs, M. Loutfy, D. Persad, and M.A. Ostrowski. 2008. Virus-specific interleukin-17-producing CD4+ T cells are detectable in early human immunodeficiency virus type 1 infection. *J. Virol.* 82:6767–6771.

18. Molesworth-Kenyon, S.J., R. Yin, J.E. Oakes, and R.N. Lausch. 2008. IL-17 receptor signaling influences virus-induced corneal inflammation. *J. Leukoc. Biol.* 83:401–408.

19. Hashimoto, K., J.E. Durbin, W. Zhou, R.D. Collins, S.B. Ho, J.K. Kolls, P.J. Dubin, J.R. Sheller, K. Goleniewska, J.F. O'Neal, et al. 2005. Respiratory syncytial virus infection in the absence of STAT 1 results in airway dysfunction, airway mucus, and augmented IL-17 levels. *J. Allergy Clin. Immunol.* 116:550–557.

20. Doherty, P.C., W. Allan, M. Eichelberger, and S.R. Carding. 1992. Roles of alpha beta and gamma delta T cell subsets in viral immunity. *Annu. Rev. Immunol.* 10:123–151.

21. Raffatellu, M., R.L. Santos, D.E. Verhoeven, M.D. George, R.P. Wilson, S.E. Winter, I. Godinez, S. Sankaran, T.A. Paixao, M.A. Gordon, et al. 2008. Simian immunodeficiency virus-induced mucosal interleukin-17 deficiency promotes *Salmonella* dissemination from the gut. *Nat. Med.* 14:421–428.

22. Guo, B., E.Y. Chang, and G. Cheng. 2008. The type I IFN induction pathway constrains Th17-mediated autoimmune inflammation in mice. *J. Clin. Invest.* 118:1680–1690.

23. Shinohara, M.L., J.H. Kim, V.A. Garcia, and H. Cantor. 2008. Engagement of the type I interferon receptor on dendritic cells inhibits T helper 17 cell development: role of intracellular osteopontin. *Immunity.* 29:68–78.

24. Sen, G.C. 2001. Viruses and interferons. *Annu. Rev. Microbiol.* 55: 255–281.

25. Intlekofer, A.M., A. Banerjee, N. Takemoto, S.M. Gordon, C.S. Dejong, H. Shin, C.A. Hunter, E.J. Wherry, T. Lindsten, and S.L. Reiner. 2008. Anomalous type 17 response to viral infection by CD8+ T cells lacking T-bet and eomesodermin. *Science.* 321:408–411.

26. Stumhofer, J.S., A. Laurence, E.H. Wilson, E. Huang, C.M. Tato, L.M. Johnson, A.V. Villarino, Q. Huang, A. Yoshimura, D. Sehy, et al. 2006. Interleukin 27 negatively regulates the development of interleukin 17-producing T helper cells during chronic inflammation of the central nervous system. *Nat. Immunol.* 7:937–945.

27. Pene, J., S. Chevalier, L. Preisser, E. Venereau, M.H. Guilleux, S. Ghannam, J.P. Moles, Y. Danger, E. Ravon, S. Lesaux, et al. 2008. Chronically inflamed human tissues are infiltrated by highly differenti-ated Th17 lymphocytes. *J. Immunol.* 180:7423–7430.

28. Dal Canto, M.C., B.S. Kim, S.D. Miller, and R.W. Melvold. 1996. Theiler's murine encephalomyelitis virus (TMEV)-induced demyelin-ation: a model for human multiple sclerosis. *Methods.* 10:453–461.

29. Brahic, M., J.F. Bureau, and T. Michiels. 2005. The genetics of the persistent infection and demyelinating disease caused by Theiler's virus. *Annu. Rev. Microbiol.* 59:279–298.

30. Hou, W., E.Y. So, and B.S. Kim. 2007. Role of dendritic cells in differ-ential susceptibility to viral demyelinating disease. *PLoS Pathog.* 3:e124.

31. Whitton, J.L., C.T. Cornell, and R. Feuer. 2005. Host and virus deter-minants of picornavirus pathogenesis and tropism. *Nat. Rev. Microbiol.* 3:765–776.

32. Pullen, L.C., S.H. Park, S.D. Miller, M.C. Dal Canto, and B.S. Kim. 1995. Treatment with bacterial LPS renders genetically resistant C57BL/6 mice susceptible to Theiler's virus-induced demyelinating disease. *J. Immunol.* 155:4497–4503.

33. Kroenke, M.A., T.J. Carlson, A.V. Andjelkovic, and B.M. Segal. 2008. IL-12– and IL-23–modulated T cells induce distinct types of EAE based on histology, CNS chemokine profile, and response to cytokine inhibi-tion. *J. Exp. Med.* 205:1535–1541.

34. Son, K.N., R.P. Becker, P. Kallio, and H.L. Lipton. 2008. Theiler's virus-induced intrinsic apoptosis in M1-D macrophages is Bax mediated and restricts virus infectivity: a mechanism for persistence of a cytolytic virus. *J. Virol.* 82:4502–4510.

35. Kolls, J.K., and A. Linden. 2004. Interleukin-17 family members and inflammation. *Immunity.* 21:467–476.

36. Lowin, B., C. Mattman, M. Hahne, and J. Tschopp. 1996. Comparison of Fas(Apo-1/CD95)- and perforin-mediated cytotoxicity in primary T lymphocytes. *Int. Immunol.* 8:57–63.

37. Jellison, E.R., S.K. Kim, and R.M. Welsh. 2005. Cutting edge: MHC class II-restricted killing in vivo during viral infection. *J. Immunol.* 174:614–618.

38. Palma, J.P., R.L. Yauch, S. Lang, and B.S. Kim. 1999. Potential role of CD4+ T cell-mediated apoptosis of activated astrocytes in Theiler's virus-induced demyelination. *J. Immunol.* 162:6543–6551.

39. Chang, J.R., E. Zaczynska, C.D. Katsetos, C.D. Platsoucas, and E.L. Oleszak. 2000. Differential expression of TGF-beta, IL-2, and other cytokines in the CNS of Theiler's murine encephalomyelitis virus-in-fected susceptible and resistant strains of mice. *Virology.* 278:346–360.

40. Jin, Y.H., M. Mohindru, M.H. Kang, A.C. Fuller, B. Kang, D. Gallo, and B.S. Kim. 2007. Differential virus replication, cytokine production, and antigen-presenting function by microglia from susceptible and re-sistant mice infected with Theiler's virus. *J. Virol.* 81:11690–11702.

41. Kang, M.H., E.Y. So, H. Park, and B.S. Kim. 2008. Replication of Theiler's virus requires NF-kappaB-activation: higher viral replication and spreading in astrocytes from susceptible mice. *Glia.* 56:942–953.

42. So, E.Y., M.H. Kang, and B.S. Kim. 2006. Induction of chemokine and cytokine genes in astrocytes following infection with Theiler's murine encephalomyelitis virus is mediated by the Toll-like receptor 3. *Glia.* 53:858–867.

43. Trottier, M., B.P. Schlitt, A.Y. Kung, and H.L. Lipton. 2004. Transition from acute to persistent Theiler's virus infection requires active viral replication that drives proinflammatory cytokine expression and chronic demyelinating disease. *J. Virol.* 78:12480–12488.

44. Wiehler, S., and D. Proud. 2007. Interleukin-17A modulates hu-man airway epithelial responses to human rhinovirus infection. *Am. J. Physiol. Lung Cell. Mol. Physiol.* 293:L505–L515.

45. Mohindru, M., B. Kang, and B.S. Kim. 2006. Initial capsid-specific CD4(+) T cell responses protect against Theiler's murine encephalomyeli-tisvirus-induced demyelinating disease. *Eur. J. Immunol.* 36:2106–2115.

46. Buljevac, D., H.Z. Flach, W.C. Hop, D. Hijdra, J.D. Laman, H.F. Savelkoul, F.G. van Der Meche, P.A. van Doorn, and R.Q. Hintzen. 2002. Prospective study on the relationship between infections and multiple sclerosis exacerbations. *Brain.* 125:952–960.

47. Correale, J., M. Fiol, and W. Gilmore. 2006. The risk of relapses in multiple sclerosis during systemic infections. *Neurology.* 67:652–659.

48. Stüve, O., and S.S. Zamvil. 1999. Pathogenesis, diagnosis, and treatment of acute disseminated encephalomyelitis. *Curr. Opin. Neurol.* 12:395–401.

49. Young, N.P., B.G. Weinshenker, and C.F. Lucchinetti. 2008. Acute disseminated encephalomyelitis: current understanding and controversies. *Semin. Neurol.* 28:84–94.

50. Numasaki, M., J.-i. Fukushi, M. Ono, S.K. Narula, P.J. Zavodny, T. Kudo, P.D. Robbins, H. Tahara, and M.T. Lotze. 2003. Interleukin-17 promotes angiogenesis and tumor growth. *Blood.* 101:2620–2627.

51. Numasaki, M., M. Watanabe, T. Suzuki, H. Takahashi, A. Nakamura, F. McAllister, T. Hishinuma, J. Goto, M.T. Lotze, J.K. Kolls, and H. Sasaki. 2005. IL-17 enhances the net angiogenic activity and in vivo growth of human non-small cell lung cancer in SCID mice through promoting CXCR-2-dependent angiogenesis. *J. Immunol.* 175:6177–6189.

52. Wong, P., and E.G. Pamer. 2003. CD8 T cell responses to infectious pathogens. *Annu. Rev. Immunol.* 21:29–70.

53. Kagi, D., F. Vignaux, B. Ledermann, K. Burki, V. Depraetere, S. Nagata, H. Hengartner, and P. Golstein. 1994. Fas and perforin path-ways as major mechanisms of T cell-mediated cytotoxicity. *Science.* 265:528–530.

54. Lowin, B., M. Hahne, C. Mattmann, and J. Tschopp. 1994. Cytolytic T-cell cytotoxicity is mediated through perforin and Fas lytic pathways. *Nature.* 370:650–652.

55. Harty, J.T., A.R. Tvinnereim, and D.W. White. 2000. CD8+ T cell effector mechanisms in resistance to infection. *Annu. Rev. Immunol.* 18:275–308.

56. van de Berg, P.J., E.M. van Leeuwen, I.J. Ten Berge, and R. van Lier. 2008. Cytotoxic human CD4(+) T cells. *Curr. Opin. Immunol.* 20:339–343.

57. You, Z., X.-B. Shi, G. DuRaine, D. Haudenschild, C.G. Tepper, S.H. Lo, R. Gandour-Edwards, R.W. de Vere White, and A.H. Reddi. 2006. Interleukin-17 receptor-like gene is a novel antiapoptotic gene highly expressed in androgen-independent prostate cancer. *Cancer Res.* 66:175–183.

58. Palmer, M.T., and C.T. Weaver. 2007. Immunology: narcissistic helpers. *Nature.* 448:416–418.

59. Nurieva, R., X.O. Yang, G. Martinez, Y. Zhang, A.D. Panopoulos, L. Ma, K. Schluns, Q. Tian, S.S. Watowich, A.M. Jetten, and C. Dong. 2007.

Essential autocrine regulation by IL-21 in the generation of inflammatory T cells. *Nature*. 448:480–483.

60. Korn, T., E. Bettelli, W. Gao, A. Awasthi, A. Jager, T.B. Strom, M. Oukka, and V.K. Kuchroo. 2007. IL-21 initiates an alternative pathway to induce proinflammatory T(H)17 cells. *Nature*. 448:484–487.

61. Barker, B.R., J.G. Parvani, D. Meyer, A.S. Hey, K. Skak, and N.L. Letvin. 2007. IL-21 induces apoptosis of antigen-specific CD8+ T lymphocytes. *J. Immunol*. 179:3596–3603.

62. Levillayer, F., M. Mas, F. Levi-Acobas, M. Brahic, and J.F. Bureau. 2007. Interleukin 22 is a candidate gene for Tmevp3, a locus controlling Theiler's virus–induced neurological diseases. *Genetics*. 176:1835–1844.

63. Kang, J.A., M. Mohindru, B.S. Kang, S.H. Park, and B.S. Kim. 2000. Clonal expansion of infiltrating T cells in the spinal cords of SJL/J mice infected with Theiler's virus. *J. Immunol*. 165:583–590.

64. Hou, W., Y. Wu, S. Sun, M. Shi, Y. Sun, C. Yang, G. Pei, Y. Gu, C. Zhong, and B. Sun. 2003. Pertussis toxin enhances Th1 responses by stimulation of dendritic cells. *J. Immunol*. 170:1728–1736.

65. Crane, M.A., C. Jue, M. Mitchell, H. Lipton, and B.S. Kim. 1990. Detection of restricted predominant epitopes of Theiler's murine encephalomyelitis virus capsid proteins expressed in the lambda gt11 system: differential patterns of antibody reactivity among different mouse strains. *J. Neuroimmunol*. 27:173–186.

66. Myoung, J., Y. Il Bahk, H.S. Kang, M.C. Dal Canto, and B.S. Kim. 2008. Anti-capsid immunity level, not viral persistence level, correlates with the progression of Theiler's virus–induced demyelinating disease in viral P1-transgenic mice. *J. Virol*. 82:5606–5617.

67. Myoung, J., W. Hou, B. Kang, M.A. Lyman, J.A. Kang, and B.S. Kim. 2007. The immunodominant CD8+ T cell epitope region of Theiler's virus in resistant C57BL/6 mice is critical for anti-viral immune responses, viral persistence, and binding to the host cells. *Virology*. 360:159–171.

68. Ivanov, I.I., B.S. McKenzie, L. Zhou, C.E. Tadokoro, A. Lepelley, J.J. Lafaille, D.J. Cua, and D.R. Littman. 2006. The orphan nuclear receptor RORgammat directs the differentiation program of proinflammatory IL-17+ T helper cells. *Cell*. 126:1121–1133.

69. Zhao, D.-M., A.M. Thornton, R.J. DiPaolo, and E.M. Shevach. 2006. Activated CD4+CD25+ T cells selectively kill B lymphocytes. *Blood*. 107:3925–3932.